

P27

強制流動沸騰における沸騰熱伝達および流動特性に及ぼす
溶存気体の影響Effect of dissolved gas on boiling heat transfer and two-
phase flow behavior in forced flow boiling榑崎裕白¹, 松本聡², 金子暁子³, 阿部豊³,Hiroaki NARAZAKI¹, Satoshi MATSUMOTO², Akiko KANEKO³, and Yutaka ABE³

1 筑波大学大学院, Department of Engineering Mechanics and Energy, University of Tsukuba#1,

2 宇宙航空研究開発機構, Japan Aerospace Exploration Agency#2,

3 筑波大学, University of Tsukuba#3,

1. Introduction

In recent years, a highly efficient cooling system is eagerly desired because of high heat flux associated with miniaturization of electronic devices and large amount of heat with upsizing of space equipment. There is a strong demand for the development of a more efficient cooling system in order to operate machines like space equipment for a long term. The heat removal performance of cooling system using flow boiling is much higher than that of the single phase flow. Thus, practical application of the cooling system using flow boiling is expected to improve cooling efficiency and downsize the system. For practical use of cooling system using flow boiling, it is necessary to deepen the knowledge on the forced flow boiling. Especially, in this study, we focused on the concentration of gas dissolved in the working fluid. Sawada et al.¹⁾ are using ISS (KIBO) to study boiling two-phase flow in a microgravity environment. Wei et al.²⁾ (2005) tested the effect of pool boiling using FC-72 as working fluid. The gas-dissolved fluid showed a decreased in the boiling incipient temperature and heat transfer performance in the low heat flux region exceeded the case of degassed fluid. However, little is known about the influence of dissolve gas on heat transfer and flow behavior in forced flow boiling.

Therefore, the purpose of this study is to clarify the effect of dissolved gas on boiling heat transfer and boiling two-phase flow behavior

2. Experiment apparatus and method

2.1 Geometry and condition of the experiment

Figure 1 shows a schematic diagram of experimental apparatus. The experimental equipment consists of pump, a preheater, a test section and a condenser, which are connected in a loop by a stainless tube with an inner diameter of 4mm and arranged horizontally. Pump pumps working fluid to circulate in loop. The preheater is used to heat the working fluid and adjust the degree of subcooling when flowing into the test section. The working fluid flowing into the test section was photographed using a high speed camera, and the temperature data was acquired by a thermocouple installed on the outer wall of the test section. The boiling two-phase flow passing through the test section becomes a liquid single-phase flow by passing through the condenser.

Table 1 shows the experiment condition in this study. Mass flux $G = 50\sim 300[\text{kg}/\text{m}^2]$ is sent by a pump, and the subcooling at the inlet of the test section was set to $\Delta T_{sub} = 10[\text{K}]$. The experiment was conducted under the conditions that the concentration of dissolved gas in the working fluid 0, 8.5, 14.1, 19.8[vol/vol%]. Perfluorohexane used as a working fluid is also used as a refrigerant and working fluid in space experiment by JAXA. Physical properties of this fluid include low boiling point ($T_{sat} = 329[\text{K}]$) and high air solubility.

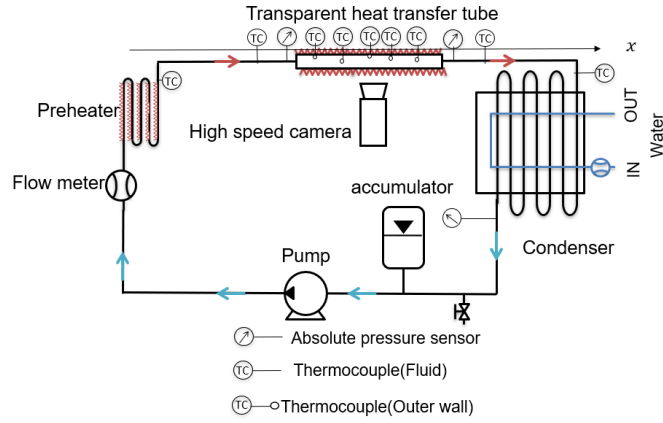


Fig.1 Experiment apparatus

Table.1 Experiment condition

Mass flux G [kg/m ² s]	50~300
Heat flux q [kW/m ²]	0~22.9
Dissolved air concentration [vol/vol%]	0, 8.5, 14.1, 19.8
Inlet pressure P_{in} [kPa]	95~103
Subcooling ΔT_{sub} [K]	10
Working fluid	Perfluorohexane
Saturation temperature T_{sat} [K]	329

2.2 Test section

Figure 2 shows a schematic diagram of the test section. A transparent heat transfer tube was used for the test section. This test section is a glass tube with an inner diameter of 4mm and a length of 50mm. The inner wall is coated with a gold thin film, and when a voltage is applied, resistance heat is generated and the working fluid can be boiled. In addition, the white LED backlight enables visualization of the boiling two-phase flow in the test section.

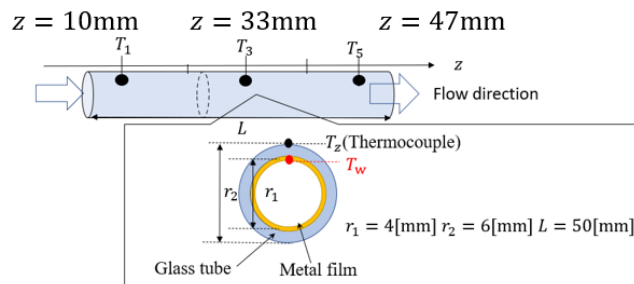


Fig.2 Test section

3. Result and discussion

3.1 Visualization result of flow boiling

Figure 3 shows the flow boiling in the test section at each mass flow rate condition. In the low mass flux condition $G = 100$ [kg/m²s], boiling bubbles like a film were formed near the heat transfer surface from the start of boiling. Under the condition of mass flux $G = 200$ [kg/m²s], bubble were generated independently and elongated bubbles were formed. When the mass flux $G = 300$ [kg/m²s], the bubbles were generated in a shape close to a sphere. As the heat flux increased, the inside of the test section area gradually became high voids, but the flow transition pattern was different for each flow rate. Especially in the condition of mass flux $G = 200$ [kg/m²s], a complicated flow pattern in which the gas-liquid interface undulated was confirmed under the condition of high heat flux.

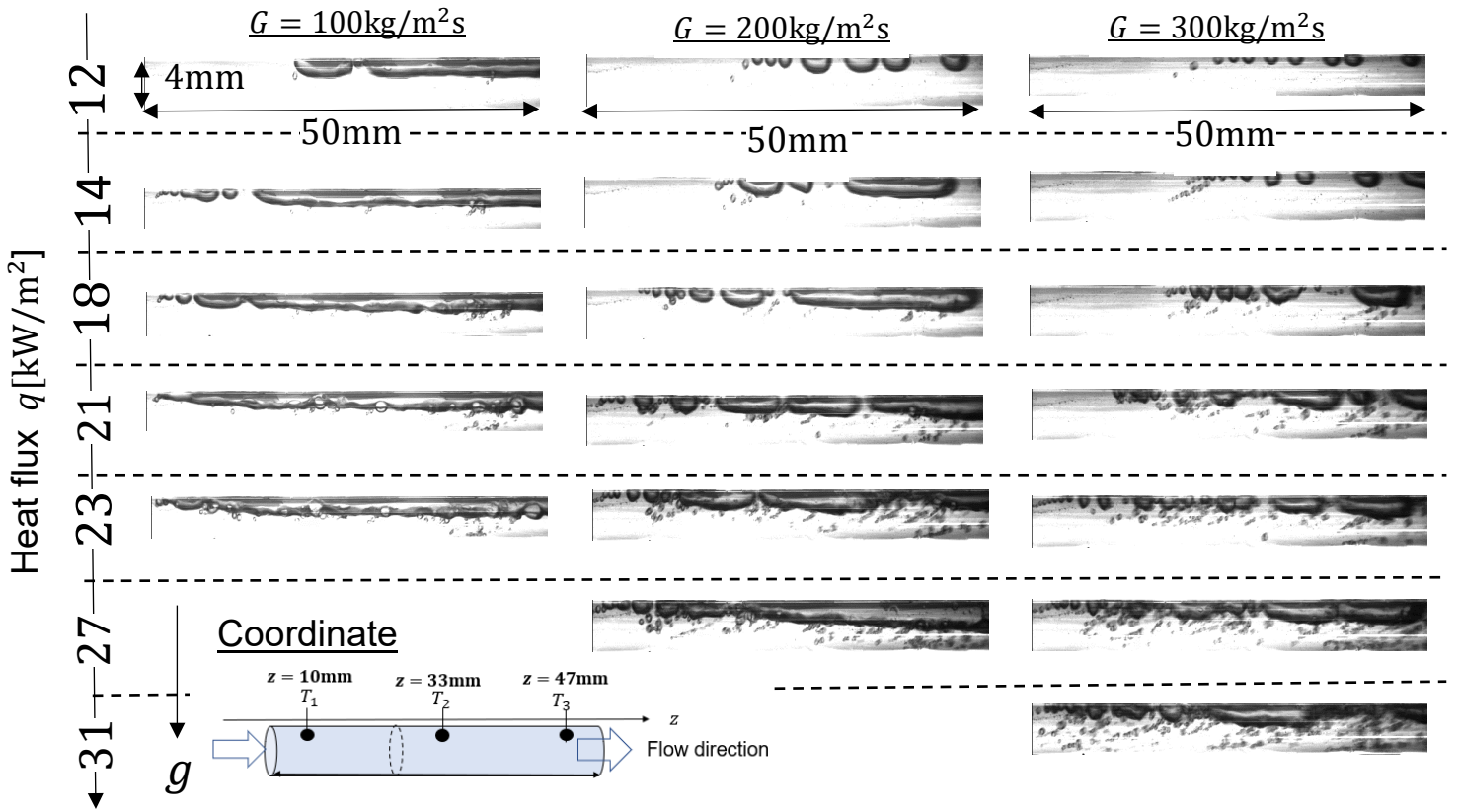


Fig.3 Visualization result of flow boiling

3.2 Temperature data of the heat transfer surface

Figure 4 shows the temperature data of the heat transfer surface for each dissolved air concentration. Under the condition of mass flow rate $G = 100$ [kg/m²s], the increasing tendency of the temperature did not change in the liquid single phase flow and the boiling two-phase flow. The effect of dissolved air was not confirmed under this condition. On the other hand, under the condition of mass flow rate $G = 200, 300$ [kg/m²s], the temperature dropped temporarily with start of boiling. In addition, boiling started at a lower temperature in the gas dissolved condition than in the undissolved condition and after boiling, the temperature rose more slowly than in case of the liquid single phase

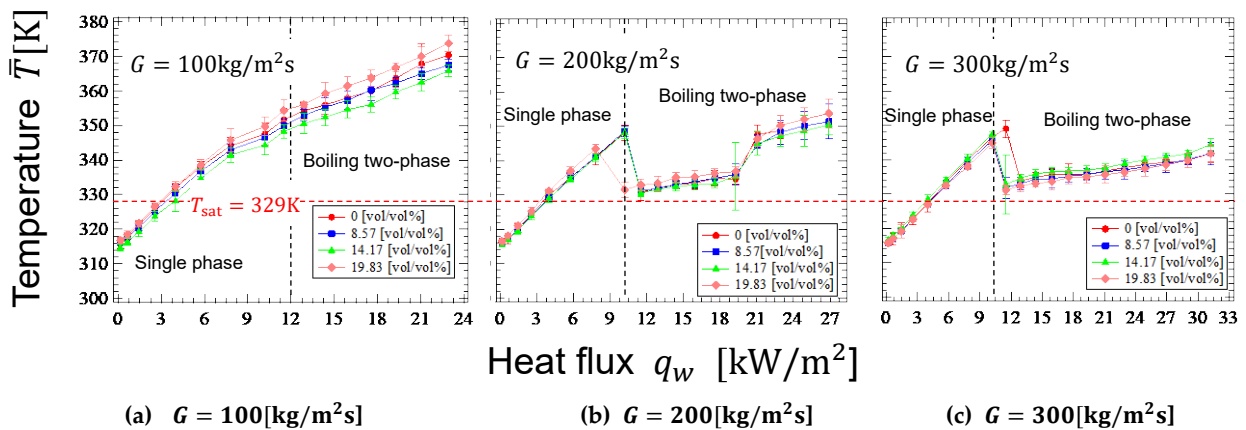


Fig.4 Temperature data

3.3 Local heat transfer coefficient

The local heat transfer coefficient at each position of the test section was calculated based on the acquired temperature data. The local heat transfer coefficient was calculated from the heat balance (Equation1).

Where, dQ is the amount of the heat in a minute section, G is a mass flow rate, C_p is a specific heat, h is a heat

$$dQ = GC_p dT = h(2\pi r L dz)(T_w - T_l) \quad (1)$$

transfer coefficient, r and L are respectively the diameter and the length of the test section, T_w and T_l are respectively temperature of test section surface and working fluid. The left side represent the heat flux that flowing from the minute section of the test section. The right side shows the amount of heat used to increase the enthalpy of the working fluid. The local heat transfer coefficient was classified into liquid single phase flow and boiling two-phase flow like Equation 2 and 3.

$$h = \frac{q}{(T_w - T_{l,z})} \quad (\text{single phase flow}) \quad (2)$$

$$h = \frac{q}{(T_w - T_{sat})} \quad (\text{two phase flow}) \quad (3)$$

Where q is heat flux and is defined by the following equation.

$$q = \frac{GAC_p(T_{out} - T_{in})}{\pi r L} \quad (4)$$

Where A is a channel cross-section area, T_{out} and T_{in} are respectively temperature of outlet and inlet of the test section. In the case of liquid single phase, the temperature of the liquid phase was calculated using Equation 4 assuming that all the heat input from the heat transfer surface is used to increase the enthalpy of the liquid phase.

$$T_{l,z} = T_{lin} + \frac{qz}{GAC_p} \quad (5)$$

Figure 5 shows the calculation result of summarizing the change in heat transfer coefficient by the dissolved gas concentration for each mass flow rate. Under the condition of the mass flux $G = 100[\text{kg}/\text{m}^2\text{s}]$, the heat transfer coefficient slightly increases as the heat flux increases. However, the value of the heat transfer coefficient was small, and the change due to the dissolved gas concentration did not occur. On the other hand, under high flow rate conditions of mass flow rate $G = 200, 300[\text{kg}/\text{m}^2\text{s}]$, the heat transfer coefficient increased as the dissolved gas concentration increased in the low heat flux region. Furthermore, under the condition of mass flux $G = 200[\text{kg}/\text{m}^2\text{s}]$, the heat transfer coefficient tended to decrease after heat flux A. From the above, it was found that the influence of dissolved gas on boiling heat transfer is remarkable especially under low quality conditions. Below, the mechanism by which the dissolved gas in the working fluid promotes boiling heat transfer will be considered.

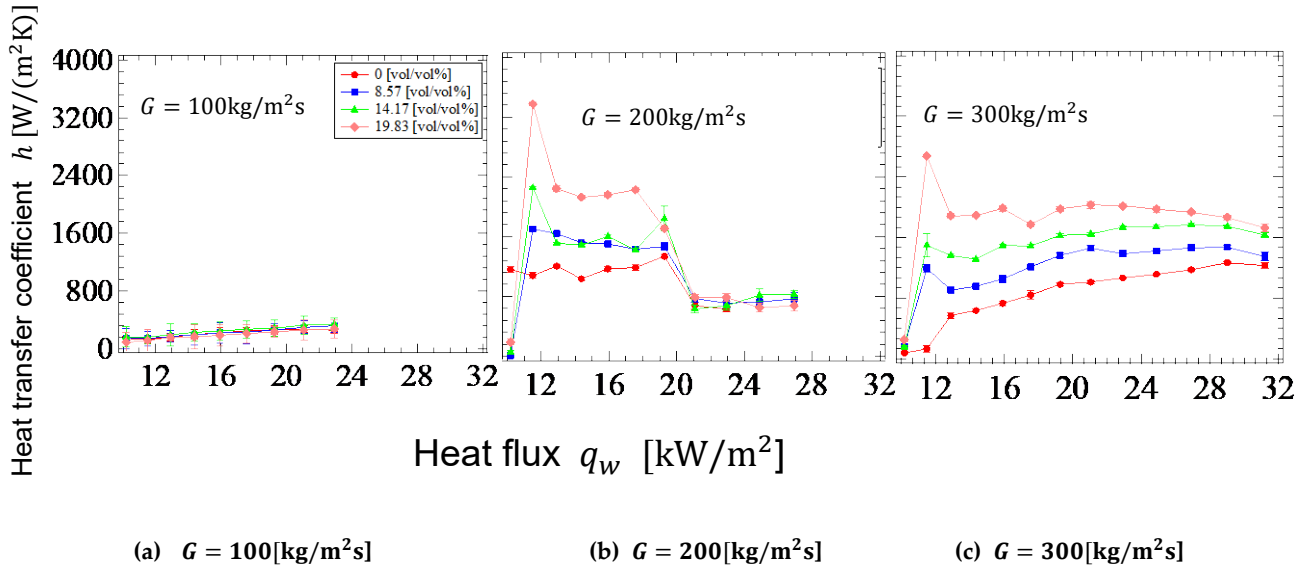


Fig.5 Heat transfer coefficient

3.4 Effect of precipitation of dissolved gas

We will describe the reason why the boiling start temperature decreases with the increase of the dissolved gas concentration under the low heat flux. **Figure 6** is result of plotting the surface area of the generated bubbles. In the degassed state, it was confirmed that the condensation rate after left the heat transfer surface tended to be higher than that in the condition in which air was dissolved. From this, it is considered that the precipitated gas plays a role as a boiling nucleus and promotes boiling under low heat flux conditions.

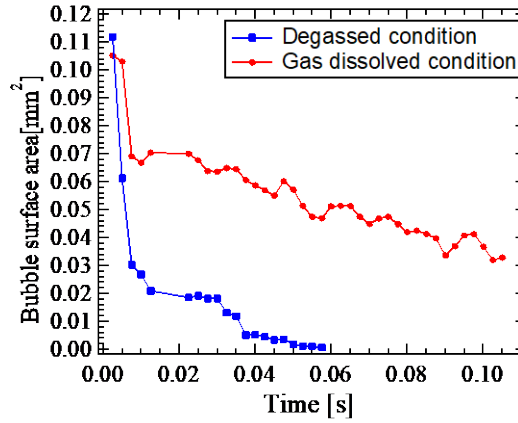


Fig.6 Bubble surface area

Figure 7 is the result of summarizing the contact angles between the generated boiling bubbles and the heat transfer surface for each dissolved gas concentration. As shown in this graph, it was confirmed that the contact angle tended to decrease as the dissolved gas concentration increased. In other words, the higher the dissolved gas concentration, the more the bubbles became flatter in the flow direction. One of the reasons for this is that the gas phase density inside the boiling bubbles is uneven. It is considered that the dissolved gas with a small gas phase density accumulated in the upper part of the boiling bubble and the vapor with a density accumulated in the lower part of the bubble, and the bubble became flat due to the influence of buoyancy.

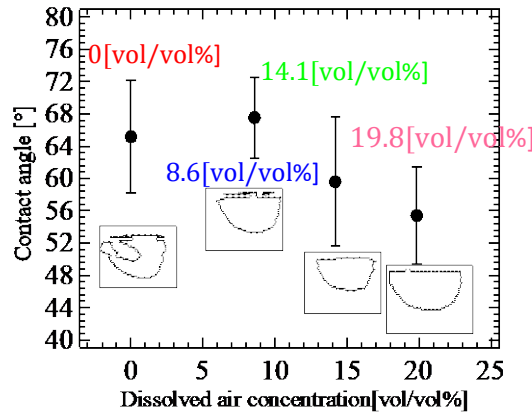


Fig.7 Contact angle

It is necessary to consider the evaporation momentum force, which is the force generated at the boiling bubble interface. Evaporation momentum force is a force generated due to the density difference between gas ρ_v and liquid ρ_l and the evaporation rate $\frac{dV_B}{dt}$. Moreover, it is said that it mainly affects the promotion of heat transfer based on pool boiling by Kandlikar et al.³⁾. The evaporation momentum force F_M is expressed by the following equation. Figure 8 shows the result of calculating the bubble volume using image processing from the visualization result of bubbles and calculating the evaporation momentum force for each gas phase density. From this result, the evaporation momentum force is larger as the bubble volume smaller and the gas phase density is larger.

$$F_M = \left(\frac{dV_B}{dt}\right)^2 \frac{\rho_v}{A_c A_B} \quad (6)$$

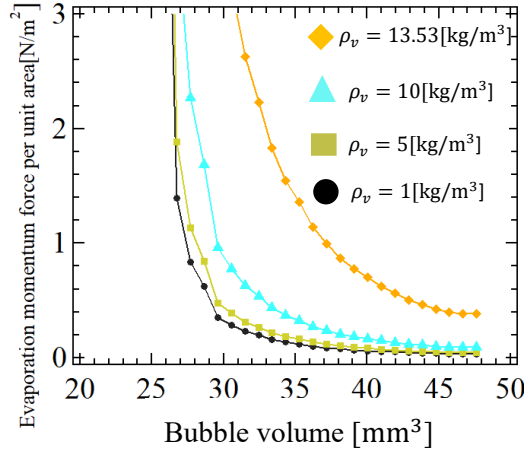


Fig.8 Evaporation momentum force

Where, V_B is the bubble volume, ρ_v is the vapor density, A_c is the channel cross section area, A_b is the bubble surface area.

The density of boiling bubbles changes and the evaporation momentum force is biased, which activates the convective motion near the heat transfer surface and supplies the amount of liquid for heat exchange. It is thought that this promoted heat transfer.

3.5 Flow pattern transition

In this chapter, we will describe the effect of dissolved gas on the flow pattern transition. Therefore, we arranged the flow patterns using a dimensionless number. The dimensionless map created this time was proposed by kim et al⁴⁾, and it is assumed that the inertial force acts predominantly on the boiling bubbles flowing in the test section. It is considered that the inertial force is predominantly exerted on the boiling bubbles even under the experimental conditions of this experiment, and it is known that the flow pattern can be accurately arranged by this map. This flow pattern map is represented using Lockhart-Martinelli parameter X_{tt} (6) on the horizontal axis and the modified Weber number We^* (7), (8) on the vertical axis.

$$X_{tt} = \left(\frac{1-x}{x}\right)^{0.9} \left(\frac{\rho_v}{\rho_l}\right)^{0.5} \left(\frac{\mu_v}{\mu_l}\right)^{0.1} \quad (7)$$

$$We^* = 2.45 \frac{Re_v^{0.64}}{Su_v^{0.3} (1 + 1.09 X_{tt}^{0.039})^{0.4}} \quad (Re_l \leq 1250) \quad (8)$$

$$We^* = 2.45 \frac{Re_v^{0.64} X_{tt}^{0.157}}{Su_v^{0.3} (1 + 1.09 X_{tt}^{0.039})^{0.4}} \left[\left(\frac{\mu_v}{\mu_l}\right)^2 \left(\frac{\rho_l}{\rho_v}\right)\right]^{0.084} \quad (Re_l > 1250) \quad (9)$$

Where, x represents the quality in the test section, and was calculated from the following equation (9) based on the temperature data at the entrance and exit of the test section.

$$x = \frac{1}{h_{lv}} \left[\frac{G A C_p (T_{out} - T_{in})}{G A} - C_p (T_{sat} - T_{in}) \right] \quad (10)$$

Figure 9 shows the result of summarizing the flow pattern for each dissolved gas concentration. The red plot is for mass flux $G = 100$ [kg/m²s], the blue plot is for mass flux $G = 200$ [kg/m²s], and the green plot is for mass flux $G = 300$ [kg/m²s]. It was found that the quality was high from the start of boiling under the condition of low mass flux $G = 100$ [kg/m²s]. In addition, the dissolved gas did not affect the flow pattern under low mass flow rate. On the other hand, in the high mass flux conditions $G = 200, 300$ [kg/m²s], the transition of the flow pattern with low quality changed with increasing the dissolved gas concentration. In other words, since boiling starts with lower quality as the dissolved air concentration increases, it is considered that the liquid phase is relatively rich in the test section during the transition process from the plug flow to slag flow. It is considered that the promotion of heat transfer coefficient as affected by the fact that a sufficient amount of liquid for heat exchange was secured.

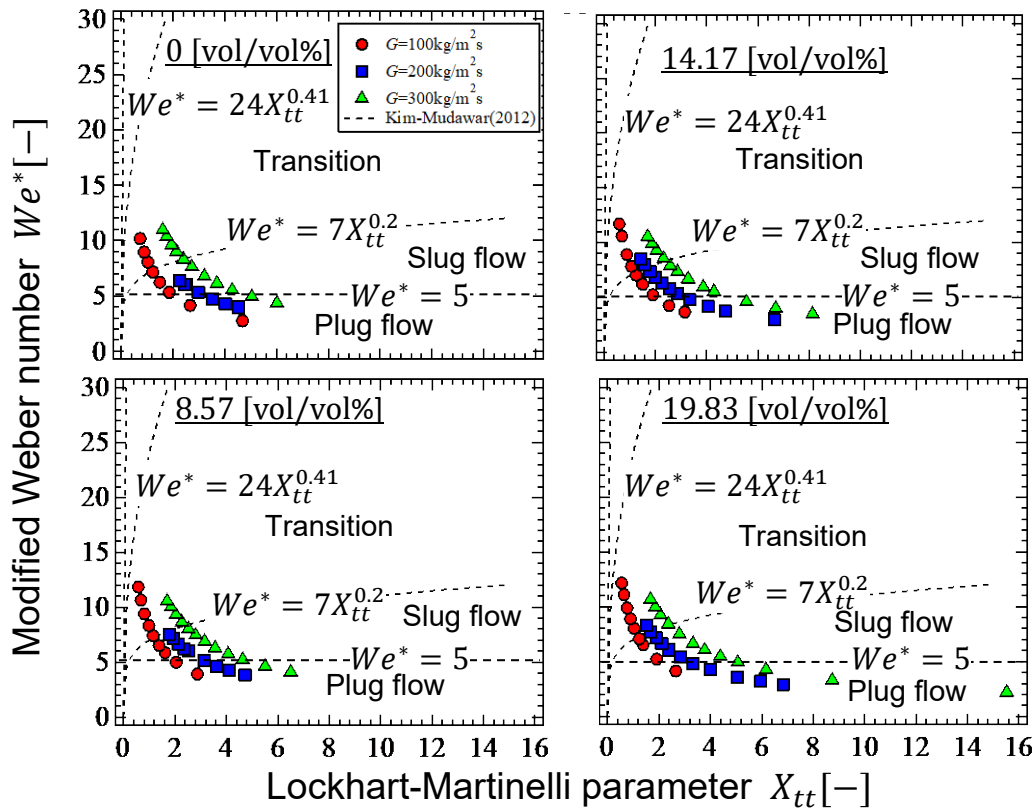


Fig.9 Flow pattern map

4. Conclusions

Visualization imaging and heat transfer measuring experiment of boiling two-phase flow were performed using transparent heat transfer tube, and the following finding were obtained.

1. Under the high quality condition where the effect of nucleate boiling appears remarkably, the effect of dissolved air did not appear on the heat transfer characteristics and flow behavior.
2. The heat transfer coefficient increased with the increase of dissolved air concentration under the low quality condition where the effect of the precipitation of air dissolved in the working fluid was remarkable.
3. It is suggested that the evaporation momentum force acting on the gas-liquid interface of boiling bubbles may promoted heat transfer in the bubbly flow region.

5. Reference

- 1) H. Ohta, S.Baba, N.Ohtani, O.Kawamura et al. Frontier in Heat and Mass Transfer Vol.3(2012)
- 2) Wei,J.J., Guo,L.J.,Honda J. Heat and Mass Transfer, Vol.41, 2005, pp.744-755.
- 3) S.G.Kandlikar., APPLIED PHYSICS LETTERS Vol.102 , 051611(2013)
- 4) Kim et al. International Journal of Heat and Mass Transfer Vol.55(2012) pp.984-994



© 2020 by the authors. Submitted for possible open access publication under the terms and conditions of the Creative Commons Attribution (CC BY) license (<http://creativecommons.org/licenses/by/4.0/>).